BNIP2 extra long inhibits RhoA and cellular transformation by Lbc RhoGEF via its BCH domain

Unice J. K. Soh and Boon Chuan Low*

Cell Signaling and Developmental Biology Laboratory, Department of Biological Sciences, National University of Singapore, 14 Science Drive 4, Singapore 117543, Republic of Singapore

*Author for correspondence (e-mail: dbslowbc@nus.edu.sg)

Accepted 13 February 2008
Journal of Cell Science 121, 1739-1749 Published by The Company of Biologists 2008
doi:10.1242/jcs.021774

Summary

Increased expression of BCH-motif-containing molecule at the C-terminal region 1 (BMCC1) correlates with a favourable prognosis in neuroblastoma, but the underlying mechanism remains unknown. We here isolated *BNIPXL* (BNIP2 Extra Long) as a single contig of the extended, in-vitro-assembled *BMCC1*. Here, we show that in addition to homophilic interactions, the BNIP2 and Cdc42GAP homology (BCH) domain of BNIPXL interacts with specific conformers of RhoA and also mediates association with the catalytic DH-PH domains of Lbc, a RhoA-specific guanine nucleotide exchange factor (RhoGEF). BNIPXL does not recognize the constitutive active G14V and Q63L mutants of RhoA but targets the fast-cycling F30L and the dominant-negative T19N mutants. A second region at the N-terminus of BNIPXL also targets the proline-rich region of Lbc. Whereas overexpression of BNIPXL reduces active RhoA levels, knockdown of BNIPXL expression has the reverse effect. Consequently, BNIPXL inhibits Lbc-induced oncogenic transformation. Interestingly, BNIPXL can also interact with RhoC, but not with RhoB. Given the importance of RhoA and RhoGEF signaling in tumorigenesis, BNIPXL could suppress cellular transformation by preventing sustained Rho activation in concert with restricting RhoA and Lbc binding via its BCH domain. This could provide a general mechanism for regulating RhoGEFs and their target GTPases.

Supplementary material available online at
http://jcs.biologists.org/cgi/content/full/121/10/1739/DC1

Key words: BNIP-2, BCH domain, Rho, RhoGEF, Lbc, Cellular transformation

Introduction

Rho proteins are part of the extensive Ras superfamily of small GTPases that cycle between inactive GDP-bound and active GTP-bound states. Despite their structural and biochemical similarities, they target different binding partners and regulate cell morphology, motility, vesicular transport, membrane trafficking, lipid signaling, cell cycle progression and gene transcription (Etienne-Manneville and Hall, 2002; Jaffe and Hall, 2005). The functions of Rho, Rac and Cdc42 have been extensively characterized (Hall, 1998). Similarly to all GTPases, they are tightly regulated by three distinct classes of protein, namely guanine-nucleotide exchange factors (GEFs), GTPase-activating proteins (GAPs) and guanine-nucleotide dissociation inhibitors (GDIs) (Bos et al., 2007). GEFs promote the exchange of GDP for GTP, GAPs stimulate intrinsic GTPase activity and GDIs inhibit nucleotide dissociation and GTP hydrolysis by sequestering Rho in inactive complexes. These regulators modulate Rho activities in response to spatio-temporal cues and may utilise their multiple domains to coordinate crosstalk between different signaling pathways (Rossman et al., 2005; Tcherkezian and Lamarche-Vane, 2007). Dysfunctional regulation of Rho signaling unsurprisingly leads to cancer (Sahai and Marshall, 2002; Ridley, 2004) and neurological disorders (Boettner and van Aelst, 2002). In addition to regulation by lipid metabolites (Rossman et al., 2005) and intrinsic phosphorylation (Moon and Zheng, 2003), it remains to be explored how the activity of these regulators on their cognate GTPases are regulated by additional cellular protein(s).

We previously identified BNIP2 and Cdc42GAP homology (BCH) domain as a conserved multi-functional protein domain, which, in addition to its ability to form homophilic and heterophilic interactions with itself or other homologous BCH domains (Low et al., 1999; Low et al., 2000a; Shang et al., 2003), has emerged as a new class of regulatory GTPase-binding domain. For example, the BNIP2 BCH domain activates Cdc42 to elicit cell protrusions (Zhou et al., 2005) whereas the BNIP-Sα BCH domain sequesters Cdc42GAP/p50RhoGAP via heterophilic BCH interactions while targeting RhoA directly for further activation, leading to apoptosis (Zhou et al., 2002; Zhou et al., 2006). Furthermore, the BCH domain of BPGAP1, a close homolog of Cdc42GAP/p50RhoGAP, also promotes Cdc42-dependent short pseudopodia, which are necessary for cell migration (Shang et al., 2003; Lua and Low, 2004) and Ras/MAPK activation (Lua and Low, 2005). More recently, we demonstrated that the BCH domain of the brain-specific BNIP-H/Caytaxin is involved in glutamate production and glutaminase trafficking (Buschdorf et al., 2006). These findings suggest that the BCH domain exerts an additional regulatory control over the cellular activity of their cognate small GTPases or other specific proteins. Identification and systematic studies of other BCH-domain-containing proteins will therefore provide further insights into the mechanistic functions of this emerging class of protein module.

We isolated the cDNA for *BNIPXL* (BNIP2 extra long) encoding a protein distinct from BNIP2 (Accession number: NP_004321). The extended isoform, BCH-motif-containing molecule at the C-terminal region 1 (BMCC1), was recently identified as a prognostic marker for childhood neuroblastomas (Machida et al., 2006). BMCC1 enhances neuronal apoptosis upon NGF depletion through as yet unknown mechanisms. Here, we show that BNIPXL could

Journal of Cell Science

Journal of Cell Science

regulate actin cytoskeletal reorganization and cellular transformation. Its BCH domain specifically targets RhoA and RhoC, but not RhoB, whereas separate pools could exist to sequester their RhoGEF, Lbc. Together, such interactions suppress primary foci formation in NIH3T3 fibroblasts. This confirms that the BCH domain acts as a regulatory GTPase-binding domain by targeting GTPases and their regulators, and could represent a general mechanism by which BNIPXL functions as an antagonist of cellular transformation.

Results

BNIPXL as a novel BCH-domain-containing protein

To identify novel BCH-domain-containing proteins, bioinformatics analyses by PSI-BLAST were conducted using full-length *Homo sapiens* BNIP2 and its BCH domain. Based on the earliest entry *KIAA0367* (Nagase et al., 1997), we isolated *BNIPXL* cDNAs that encode a 769 amino acid (*BNIPXLα*; accession number, AY439213) and a 732 amino acid protein (*BNIPXLβ*; accession number, AY439214). The shorter variant results from alternative splicing of exons 11 and 12, which introduces an in-frame stop codon (supplementary material Fig. S1). Multiple sequence analyses of BNIPXL with four other BCH-containing proteins that we previously identified – BNIP2, BNIP-Sα, BNIP-H/Caytaxin and BPGAP1 – indicates the closest homology to BNIP2 across the entire protein (58% identity, 74% similarity) (Fig. 1A), whereas its BCH domain is most similar to that of BNIP-H/Caytaxin (76% identity, 90% similarity) (Fig. 1B and supplementary material Fig. S2). To prevent crosshybridization arising from their significant similarities to *BNIP2* and other BCH-domain-containing homologs, and to effectively distinguish *BNIPXLα* expression from *BNIPXLβ*, semi-quantitative RT-PCR using specific primers spanning the alternative splice sites demonstrate that both transcripts are expressed in all tissues and cell lines examined except in kidney HEK293T cells, where only the *BNIPXLβ* isoform was detectable (supplementary material Fig. S3). Recently, Machida et al. (Machida et al., 2006) assembled several cDNA fragments, which together encode a much-extended form, *BMCC1*. However, in our cell types and culture conditions, we were unable to isolate any sequences upstream of *BNIPXL* in a single contig or detect the endogenous 350 kDa protein expected of BMCC1 in HEK293T cells, as previously described (Machida et al., 2006). A further MEGABLAST (optimized for highly similar sequences) search using the *BMCC1* coding sequence as query against the human expressed sequence tag (EST) database revealed that a 1.5 kb region upstream of *BNIPXL* was not represented by any ESTs (data not shown). These results imply that *BNIPXL* could represent another isoform of the BMCC gene family that is differentially expressed. Here, we set out to explore the mechanistic roles of the BMCC gene family by directly investigating how the prototypical BNIPXL engages its cellular protein partners to regulate cell growth.

BNIPXL BCH domain associates with RhoA and RhoC, but not RhoB, and elicits cell morphological changes

Our previous work indicates that the BNIP2 BCH domain activates Cdc42 for cell protrusions (Zhou et al., 2005) whereas BNIP-Sα targets RhoA and Cdc42GAP/p50RhoGAP, leading to concerted RhoA activation and apoptosis (Zhou et al., 2002; Zhou et al., 2006). Phylogenetic analyses indicate that the BNIPXL BCH domain is highly homologous to that of BNIP2 and BNIP-Sα (supplementary material Fig. S2), raising the possibility that BNIPXL could also associate with Rho subfamily GTPases and

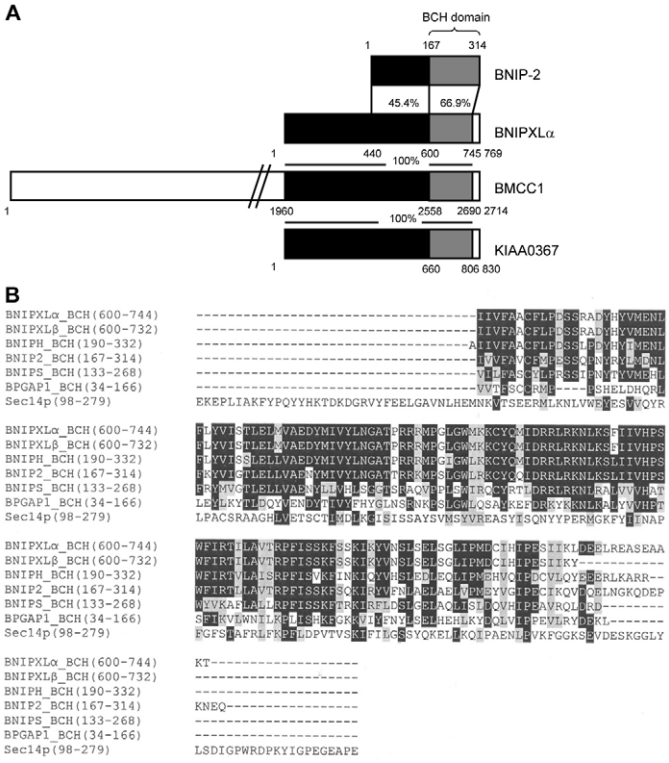

Fig. 1. BNIPXL is a novel BCH-domain-containing protein. (A) Schematic diagram showing pairwise comparisons of BNIPXLα with BNIP2, BMCC1 and KIAA0367. The BCH domain and conserved regions are shaded in gray and black, respectively. Values represent percentage amino acid identity. (B) Multiple sequence alignments of BCH domains from *H. sapiens* BNIPXLα (AY439213), BNIPXLβ (AY439214), BNIP2 (NP_004321), BNIPSα (AY078983), BNIPH (AAO63019), BPGAP1 (AF544240) and *Saccharomyces cerevisiae* Sec14p lipid-binding domain (P24280) using ClustalW and formatted using BOXSHADE. Identical residues are shaded black whereas those that are similar or conserved are gray.

regulate their biological functions. To test this hypothesis, cells were transfected with Flag-BNIPXL (Fig. 2A) and HA-RhoA or HA-Cdc42 and immunoprecipitated with anti-Flag beads. Bound proteins were resolved for anti-HA western analyses. The results confirmed that both BNIPXL isoforms could indeed interact with RhoA but not with Cdc42 (Fig. 2B). RhoA, RhoB and RhoC are three highly related (sharing 85% identity), but play distinct roles in cells (Wheeler and Ridley, 2004). RhoA participates in oncogenic transformation, whereas RhoC promotes tumor metastasis and cell migration (Wang et al., 2003; Wu et al., 2004; Ridley, 2004; Hakem et al., 2005). By contrast, RhoB is predominantly involved in endosome trafficking (Fernandez-Borja et al., 2005). To examine the functional role(s) of BNIPXL, we determined the specificity of its BCH domain toward these Rho proteins. Coimmunoprecipitation studies with HA-Rho isoforms showed that the CBCH (contains BCH) fragment of BNIPXLβ is highly specific to RhoA and RhoC (Fig. 2C). No binding was observed with other regions of BNIPXL (Fig. 3). Finally, we show that the CBCH fragment but not the N-terminus WBCH (without BCH) or the shorter NBCH (no BCH) fragments of BNIPXL could readily bind to full-length BNIPXLβ (Fig. 2D). This observation confirms that the BNIPXL BCH domain, like all other BCH domains, forms homophilic complexes, adding to the versatility of this protein-protein interaction module. Collectively, these results support the

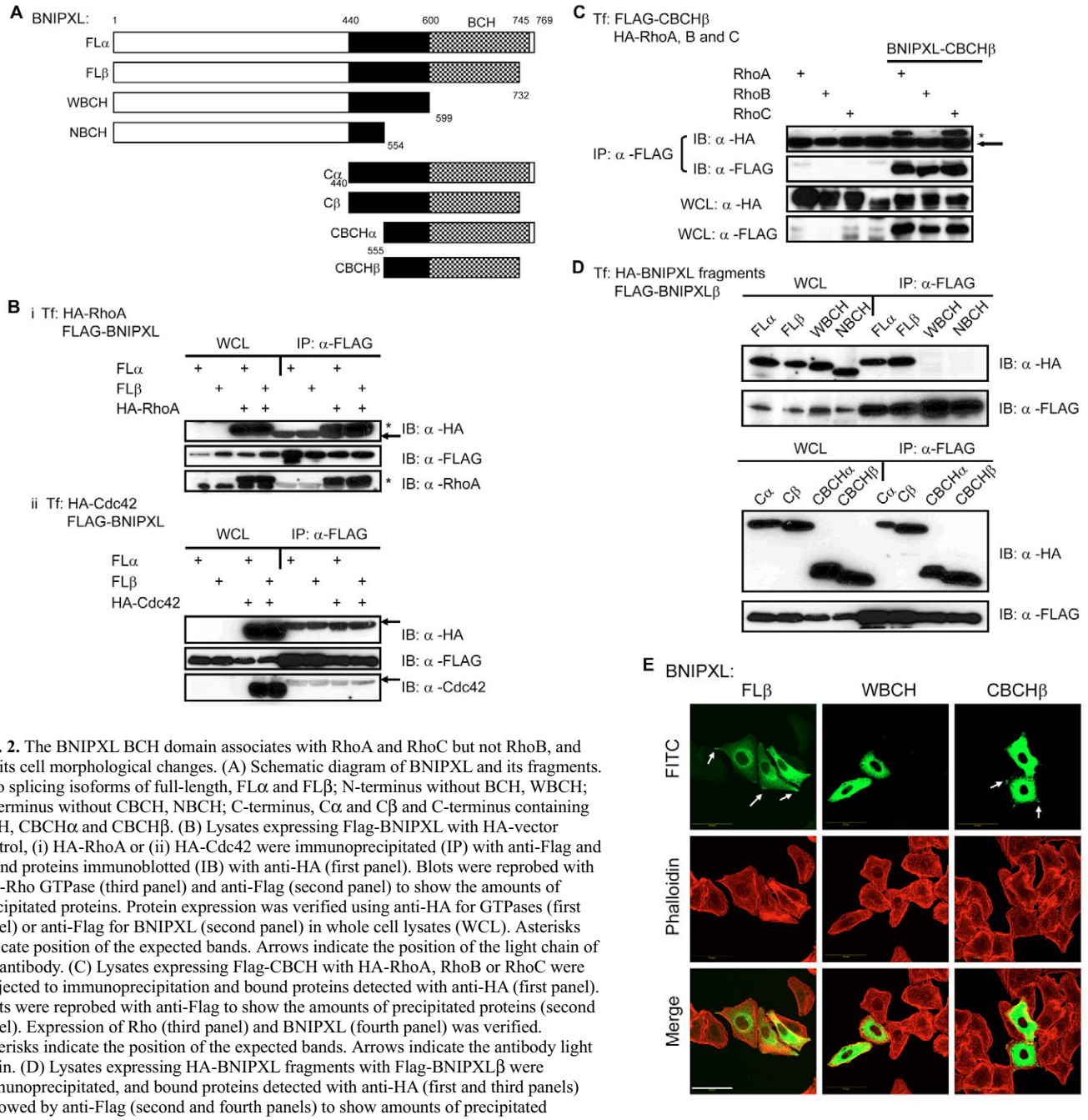

Fig. 2. The BNIPXL BCH domain associates with RhoA and RhoC but not RhoB, and elicits cell morphological changes. (A) Schematic diagram of BNIPXL and its fragments. Two splicing isoforms of full-length, FLα and FLβ; N-terminus without BCH, WBCH; N-terminus without CBCH, NBCH; C-terminus, Cα and Cβ and C-terminus containing BCH, CBCHα and CBCHβ. (B) Lysates expressing Flag-BNIPXL with HA-vector control, (i) HA-RhoA or (ii) HA-Cdc42 were immunoprecipitated (IP) with anti-Flag and bound proteins immunoblotted (IB) with anti-HA (first panel). Blots were reprobed with anti-Rho GTPase (third panel) and anti-Flag (second panel) to show the amounts of precipitated proteins. Protein expression was verified using anti-HA for GTPases (first panel) or anti-Flag for BNIPXL (second panel) in whole cell lysates (WCL). Asterisks indicate position of the expected bands. Arrows indicate the position of the light chain of the antibody. (C) Lysates expressing Flag-CBCH with HA-RhoA, RhoB or RhoC were subjected to immunoprecipitation and bound proteins detected with anti-HA (first panel). Blots were reprobed with anti-Flag to show the amounts of precipitated proteins (second panel). Expression of Rho (third panel) and BNIPXL (fourth panel) was verified. Asterisks indicate the position of the expected bands. Arrows indicate the antibody light chain. (D) Lysates expressing HA-BNIPXL fragments with Flag-BNIPXLβ were immunoprecipitated, and bound proteins detected with anti-HA (first and third panels) followed by anti-Flag (second and fourth panels) to show amounts of precipitated proteins. Protein expression was verified with anti-HA (first and third panels) and anti-Flag (second and fourth panels), respectively. (E) HeLa cells expressing Flag-BNIPXL fragments in normal growth medium were fixed 24 hours post transfection and stained as indicated. F-actin was detected with TRITC-conjugated phalloidin and cells were visualized by confocal fluorescence microscopy. Arrows indicate membrane protrusions and protein concentrated at the tips of protrusions. Scale bar: 50 μm.

notion that the BNIPXL BCH domain is a novel Rho-targeting domain and is likely to be involved in Rho-mediated cellular processes. Consistently, HeLa cells expressing full-length BNIPXLβ and the CBCH fragment induced short membrane protrusions to which they are highly localized – in addition to being perinuclear and punctate in the cytosol (Fig. 2E, arrows). By contrast, the WBCH fragment presented a uniform cytosolic distribution with no distinct change in cell morphology. Since BNIPXL targets RhoA, such subtle morphological changes imply the possible involvement of RhoA downstream of BNIPXL.

BNIPXL binds to specific RhoA conformers

We further investigated the molecular basis and functional significance of BNIPXL-Rho interaction by focusing on RhoA and BNIPXLβ (since similar results were observed for BNIPXLα). To confirm that BNIPXLβ-RhoA interaction was indeed direct, in vitro transcribed and translated Flag-BNIPXL was incubated with equal amounts of bacterially produced GST or GST-RhoA after guanine nucleotide depletion. The results indicate that the CBCH but not the WBCH fragment forms direct and enhanced interactions with RhoA, whereas full-length BNIPXL interactions with RhoA could

be detected only after prolonged film exposure (Fig. 3A). However, no signals were detected for the negative control and WBCH fragment even after prolonged exposure, suggesting that the BNIPXL N-terminus could exert an autoinhibitory effect, restricting BNIPXL-RhoA interaction. Next, we examined whether BNIPXL could interact with different RhoA conformers. GST-RhoA was unloaded or loaded with GDP or GTPγS (a non-hydrolyzable GTP analogue), and incubated with lysates expressing BNIPXL WBCH, CBCH fragments or p160ROCK, a RhoA effector (Ishizaki et al., 1996) used as a positive control for GTP-RhoA loading (Fig. 3B). Unlike p160ROCK binding, which is strictly specific to active GTP-Rho, the BNIPXL CBCH fragment has no distinct preference for the nucleotide-free or GTPγS-RhoA, although less so for GDP-RhoA. The BNIPXL WBCH fragment was not precipitated by any of the RhoA conformers. These results suggest that the BCH domain could be sensitive towards specific RhoA conformations in vivo, requiring specific regions or motifs. To probe this further, BNIPXL interaction with RhoA constitutive active and dominant negative mutants was examined in vivo. The constitutive active G14V and Q63L mutants or the 'fast-cycling' F30L mutant cause a net increase in active RhoA. G14V and Q63L are locked in an active conformation mimicking GTP-RhoA in vitro, because residues for GAP recognition in the P-loop (residues 12-19) and switch II (residues 62-68) regions have been mutated (Dvorsky and Ahmadian, 2004; Bos et al., 2007). By contrast, F30L is spontaneously active and demonstrates enhanced GDP to GTP exchange, while retaining regular GTP hydrolysis rates catalyzed by GAPs (Lin et al., 1999). The dominant negative T19N mutant

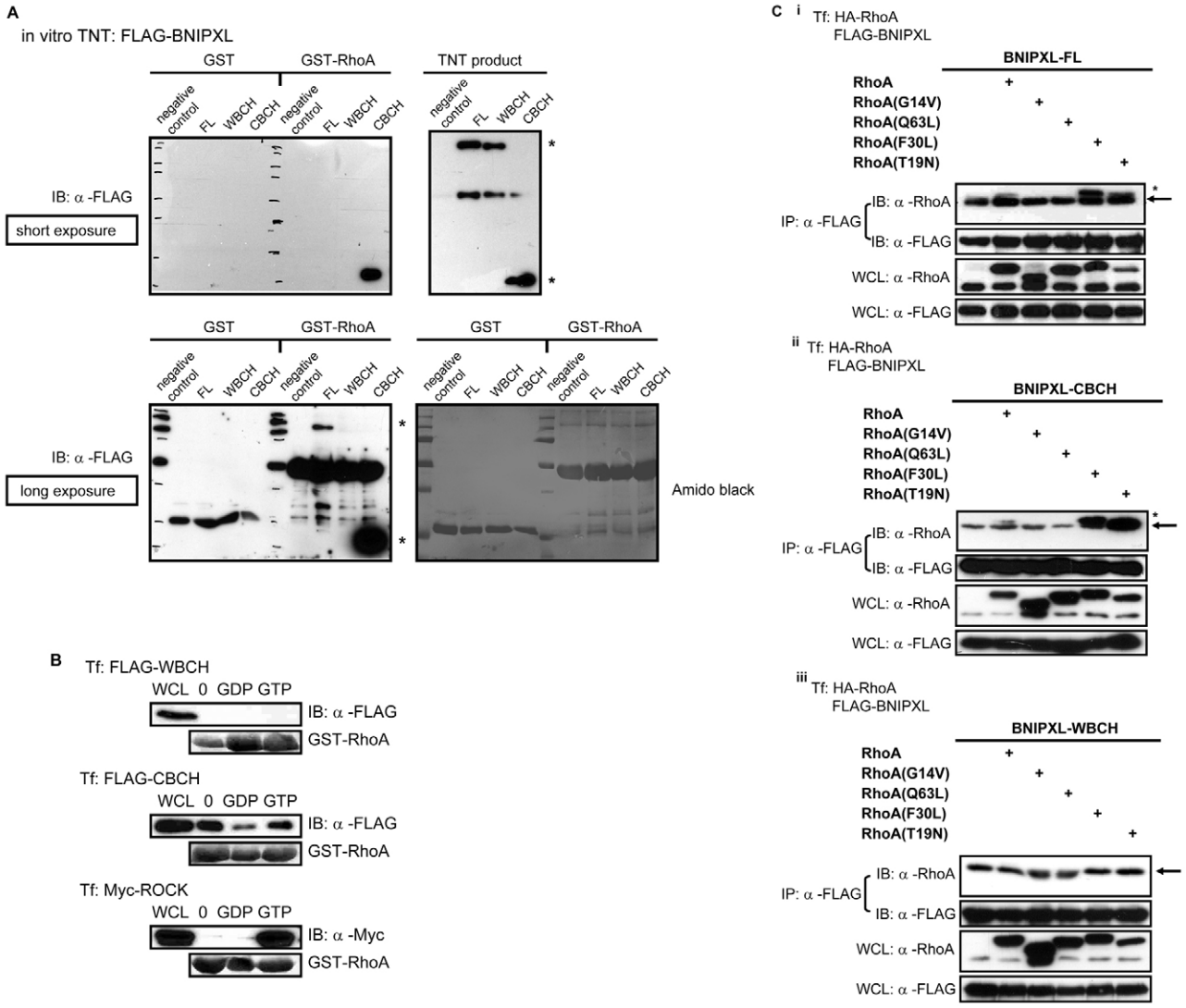

Fig. 3. BNIPXL binds to specific RhoA conformers. (A) Flag-BNIPXL full-length and fragments were transcribed and translated in vitro and incubated with GST or GST-RhoA (free of guanine nucleotides). Bound proteins were subjected to anti-Flag western blotting for short (30 seconds) and long (1 hour) exposure times. Amido Black staining was used to ascertain equal loading of GST fusion proteins. Asterisks indicate positions of the expected bands. (B) HEK293T lysates expressing Flag-BNIPXL fragments were incubated with unloaded GST-RhoA, GST-RhoA preloaded with GDP or GTPγS. Bound proteins and WCL input were analyzed with anti-Flag or anti-Myc before Amido Black staining. (C) Lysates expressing Flag-BNIPXL (i) full-length, (ii) CBCH or (iii) WBCH fragments with vector control, HA-RhoA wild type or mutants were subjected to immunoprecipitation and bound proteins detected with anti-RhoA (first panel). Blots were reprobed with anti-Flag to show the amounts of precipitated proteins (second panel). Expression of RhoA (third panel) and BNIPXL (fourth panel) was verified. Asterisks indicate position of the expected bands. Arrows indicate position of the antibody light chain.

Journal of Cell Science

Journal of Cell Science

on the other hand, sequesters and inhibits multiple endogenous RhoGEFs, preventing RhoA activation leading to elevated GDP-RhoA levels in vivo. Coimmunoprecipitation of cells transfected with Flag-BNIPXL, CBCH or WBCH fragments and HA-RhoA wild-type or mutants show that the full-length BNIPXL and the BNIPXL CBCH fragment associate weakly with wild-type RhoA, and this was greatly enhanced with the F30L or T19N mutants (Fig. 3C). In strong contrast to the GDP/GTP loading experiments, the G14V or Q63L mutants did not interact with BNIPXL or CBCH, despite being locked in the GTP-bound conformation. Although such preference is not observed in vitro, these results are likely to reflect the greater affinity between BNIPXL and GDP-RhoA in vivo. As a negative control, the WBCH fragment fails to associate with any RhoA conformers. This is consistent with a survey of RhoA structural motifs indicating the importance of the P-loop region for effector binding and GAP recognition (Dvorsky and Ahmadian, 2004). Interestingly, the same regions are important for GEF recognition and nucleotide dissociation (Bos et al., 2007). Taken together, these results demonstrate that the BNIPXL BCH domain can detect RhoA conformational changes, most likely by targeting its P-loop and switch II regions.

Interaction of BNIPXL with RhoA requires an intact BCH domain

We next examined whether the BNIPXL BCH domain contains a unique motif(s) for binding RhoA. Our previous report indicates that the BNIP-Sα BCH domain contains a RhoA-binding domain (RBD) (residues 148-177) (Zhou et al., 2006). Multiple sequence alignments of class I Rho-binding motifs found in several RhoA effectors (Fujisawa et al., 1998) and the BNIP-Sα RBD motif suggests that the proximal region of the BNIPXL BCH domain (residues 615-644) could be important for RhoA binding (supplementary material Fig. S4). A series of three BNIPXL internal deletions (designated Δ0, Δ1 and Δ2) flanking the putative RhoA-binding motif was generated after considering its secondary structure (Fig. 4A, panel i). To minimize disruption of important folds, residues outside the putative α-helices were chosen to define the deletions. Coimmunoprecipitation of lysates expressing these deletions and wild-type RhoA demonstrates that any deletion spanning these regions disables BNIPXL-RhoA binding (Fig. 4A, panel ii). To ensure that the structural integrity and native cellular distribution of these deletions were not altered, they were tested for their ability to form homophilic interactions with wild-type BNIPXL (Fig. 4B). Similarly, these mutants retained a cytosolic distribution when transiently expressed in HeLa cells (supplementary material Fig. S5). These results therefore suggest that multiple motifs within the BCH domain are essential for RhoA recognition.

BNIPXL suppresses RhoA activity and stress fiber formation in vivo

The observation that BNIPXL binds specifically to distinct RhoA mutants, which have altered levels of steady-state GTP-RhoA implies that BNIPXL could directly or indirectly affect RhoA activity. To examine this, RBD pull-down assays were performed to determine active RhoA levels in HEK293T cells expressing the wild-type, Q63L or F30L RhoA mutants in the absence or presence of wild-type BNIPXL or its deletions. To show the efficacy of this assay (Fig. 4C, panel i), GST-RBD greatly precipitated both active Q63L and F30L compared with wild-type RhoA and did not bind T19N. The levels of active wild-type RhoA were greatly reduced in the presence of BNIPXL. Strikingly, the non-interactive mutants (Δ0, Δ1 and Δ2) could also reduce active RhoA levels, but only by 50% (Fig. 4C, panel ii). By contrast, the active Q63L level was not affected, because BNIPXL could not bind to this specific form (Fig. 3C). Consistently, wild-type BNIPXL reduced the overall level of active F30L, albeit less effectively than wild-type RhoA. This is probably because the fast-cycling mutant can counteract the inhibition with its greater intrinsic rate of GDP-GTP exchange. By comparison, the noninteractive mutants of BNIPXL failed to reduce the active F30L levels.

If BNIPXL can indeed reduce active RhoA levels, then suppression of BNIPXL expression should increase Rho-GTP loading. To verify this, short hairpin RNA (shRNA) was used to transiently knockdown BNIPXL expression in 293T cells. Of the six shRNAs used, the sh470 construct demonstrated effective knockdown of HA-BNIPXL expression without affecting endogenous RhoA levels (Fig. 4D, panel i). RBD pull-down assay was performed using lysates cotransfected with wild-type RhoA and sh470 or with two other non-targeting shRNA sequences (sh484 and sh47C). In strong contrast to the ability of BNIPXL to reduce GTP-RhoA levels, transient expression of sh470 but not sh484 and sh47C resulted in an increase in active RhoA levels. Collectively, these results suggest that BNIPXL acts as an upstream and negative regulator of RhoA.

RhoA activation promotes actin stress fibers in many cell types. The effect of BNIPXL and its deletion mutants on stress fiber formation was examined in serum-stimulated NIH3T3 fibroblasts. The extent of transfected cells exhibiting stress fibers was scored and indicated that 50% of cells expressing full-length BNIPXL had reduced phalloidin staining, consistent with its inhibition of RhoA activity. Representative fields of cells are shown in Fig. 4E, panel i. However, similar to the partial inhibition on RhoA activity in the RBD pull-down assays, we observed that a small percentage (25-30%; $P<0.01$) of cells expressing the deletion mutants that failed to interact with RhoA still exhibited some degree of inhibition on stress fiber formation at a lower potency (Fig. 4E, panel ii). Taken together, these results imply that BNIPXL could exert inhibition on RhoA activity directly by binding through its BCH domain and also via an additional mechanism that could be independent of such an interaction.

BNIPXL targets endogenous proto-Lbc, a RhoA-specific GEF, and suppresses its transforming activity

Since BNIPXL binds RhoA to reduce overall intracellular RhoA activity, it remains unclear whether such binding would only sequester RhoA, thus preventing activation by its upstream activators (such as Rho GEFs) or sequester both RhoA and the immediate RhoGEF from interacting with one another. Several indirect lines of evidence provide clues for the likelihood that BNIPXL could at least prevent RhoA binding to RhoGEF, while at the same time targeting a RhoGEF independently of RhoA binding. First, the BNIPXL BCH domain has a unique binding profile not commonly seen in any RhoGEFs or RhoGAPs. The ability of BNIPXL to recognize unbound and GTP-bound RhoA could indicate the possible sequestration of free RhoA from guanine-nucleotide exchange or for promoting subsequent GTP hydrolysis. Second, it associates strongly with RhoA-T19N, a mutant that serves to target RhoGEFs in a dominant-negative manner. Thus, BNIPXL could potentially compete with RhoGEF binding to RhoA. Third, although BNIPXL reduced GTP-RhoA levels and stress fiber formation, its deletion mutants that failed to interact with RhoA could still partially exert such inhibitory effects, indicative of a mechanism that is independent of direct RhoA binding. To address these

Journal of Cell Science

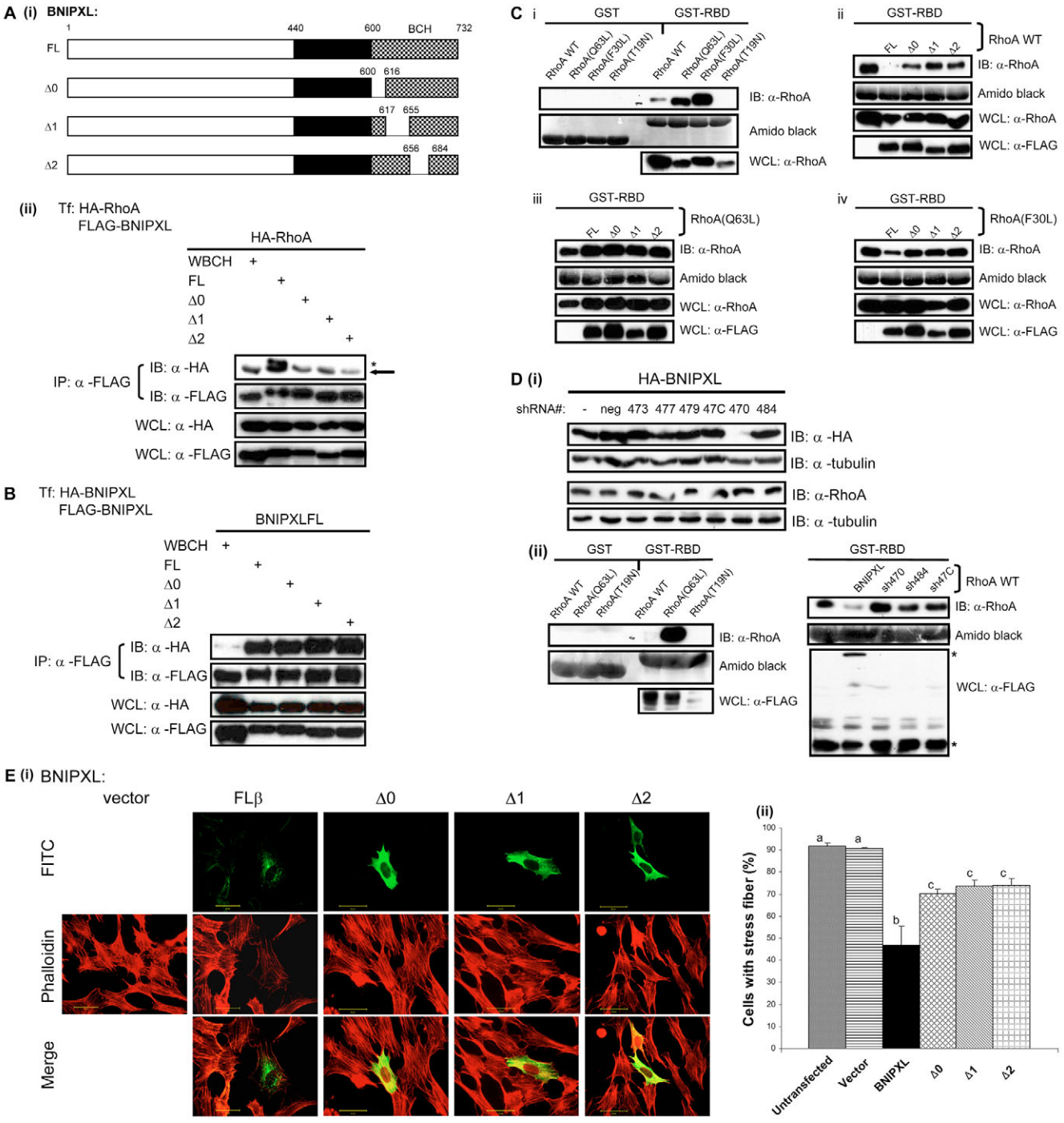

Fig. 4. See next page for legend.

possibilities, we adopted a candidate approach and examined whether BNIPXL could interact with the RhoA-specific GEF, proto-Lbc. The Lbc (lymphoid blast crisis) oncogene (Toksoz and Williams, 1994), Lfc (first cousin of Lbc) (Whitehead et al., 1995), and the mouse homologue of p115RhoGEF, Lsc (second cousin of Lbc) (Whitehead et al., 1996) are a subgroup of the Dbl (diffuse B-cell lymphoma) family GEFs that exhibit specificity toward Rho (Hart et al., 1994; Zheng et al., 1995; Glaven et al., 1996). Interestingly, our results show that BNIPXL and BMCC1 could associate with proto-Lbc as observed in coimmunoprecipitation studies (supplementary material Fig. S6). Interestingly, BNIPXL and BNIP-Sα are the only BNIP2 family members that target proto-Lbc (Fig. 5A). To determine whether BNIPXL interacts endogenously with proto-Lbc, we immunoprecipitated Flag-BNIPXL in 293T cells and assayed for the presence of endogenous proto-Lbc in the immunoprecipitates. We demonstrated that BNIPXL could indeed form a complex with endogenous proto-Lbc under normal growth conditions, albeit weakly (Fig. 5B).

To identify the binding regions on proto-Lbc, a series of proto-Lbc truncations were generated, as previously described (Sterpetti

Journal of Cell Science

Fig. 4. BNIPXL-RhoA interaction requires an intact BCH domain and reduces active RhoA levels and serum-induced stress fiber assembly. (Ai) Schematic diagram of BNIPXL internal deletions: Δ0 (Δ600-616), Δ1 (Δ617-655) and Δ2 (Δ656-684). All numbers are inclusive. Lysates expressing Flag-BNIPXL full-length, WBCH, Δ0, Δ1 and Δ2 with (Aii) HA-RhoA or (B) HA-BNIPXL were immunoprecipitated and probed with anti-HA (first panel) and reprobed with anti-Flag (second panel) to show the amounts of precipitated proteins. Protein expression was verified with anti-HA (third panel) and anti-Flag (fourth panel). The asterisk indicates the position of the expected bands. Arrow indicates the position of the light chain from antibody. (C) Lysates expressing (i) wild-type RhoA, Q63L, F30L or T19N mutants were incubated with GST or GST-RBD to confirm the specificity of the GST-RBD. Lysates expressing Flag-BNIPXL full-length or deletions with (ii) wild-type RhoA, (iii) Q63L or (iv) F30L mutants were incubated with GST-RBD. Bound proteins and WCL were analyzed using anti-RhoA (first and third panels, respectively) or anti-Flag for BNIPXL (fourth panels) before Amido Black staining to ascertain equal loading (second panels). (Di) 293T cells cotransfected with HA-BNIPXL and the shRNA constructs or scrambled negative control was lysed 72 hours post-transfection and subjected to anti-HA (100 μg WCL) (first panel) or anti-RhoA (50 μg WCL) (third panel) westerns to determine the extent of expression knockdown and endogenous RhoA levels, respectively and normalized against anti-tubulin (second and fourth panels). (Dii) 293T cells coexpressing wild-type RhoA, Q63L or T19N mutants were incubated with GST or GST-RBD to confirm the specificity of GST-RBD. Lysates expressing Flag-RhoA wild type with Flag-BNIPXL or the shRNA constructs were incubated with GST-RBD. Bound proteins and WCL were analyzed using anti-RhoA (first panel) or anti-Flag (third panel) to determine protein expression. Amido Black staining was used to ascertain equal loading of GST fusion proteins (second panel). Asterisks indicate position of expected bands. (Ei) Representative fields of NIH3T3 expressing full-length BNIPXL and BNIPXL deletions were starved 24 hours post transfection for 16 hours and stimulated with 0.5% serum-containing growth medium for 10 minutes. Cells were fixed, stained and visualized by immunofluorescence. Scale bars: 20 μm. (Eii) For quantitative analysis, the ratio of transfected cells with and without stress fibers was scored and at least 100 transfected cells were counted per sample per experiment. Data are means ± s.d. (n=3). Differences between values not sharing the same letters (a, b, c) are statistically significant at P<0.01 by analysis of variance and the Student-Newman-Keuls multiple range test (Statgraphics).

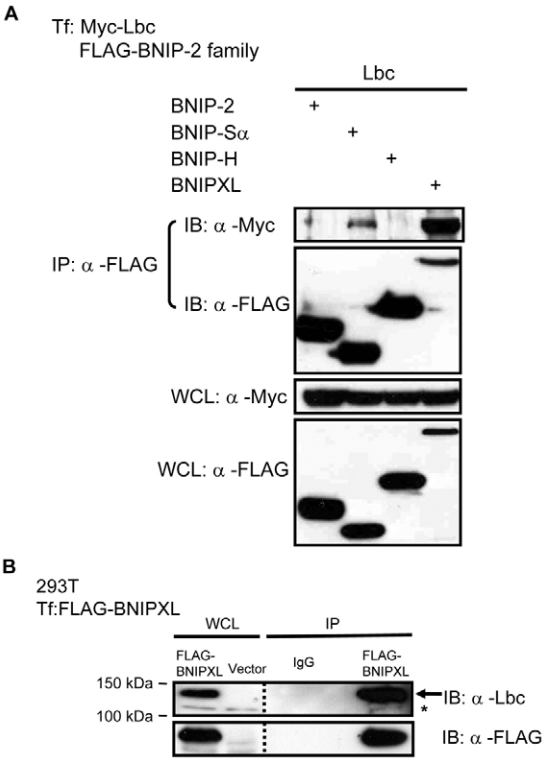

Fig. 5. BNIPXL is a specific member of the BNIP2 family that interacts with Lbc. (A) HEK293T lysates expressing Flag-BNIPXL, BNIP2, BNIP-Sα and BNIP-H with Myc-proto-Lbc were immunoprecipitated, and bound proteins detected with anti-Myc (first panel) and anti-Flag (second panel) to show the amounts of precipitated proteins. Expression of Lbc (third panel) and BNIPXL (fourth panel) was verified. (B) Equal amounts of WCL expressing vector control or Flag-BNIPXL were immunoprecipitated, and bound proteins detected with anti-Lbc (first panel). Blots were probed with anti-Flag (second panel) to verify protein expression and precipitation. Asterisk indicates position of the expected band. Arrow indicates nonspecific bands arising from anti-Lbc antibody.

et al., 1999) (Fig. 6A), and used in coimmunoprecipitations with BNIPXL (Fig. 6B-E). Full-length BNIPXL bound to all the truncation mutants, although relatively weak interactions were detected with PS. Interestingly, different binding profiles were observed with the CBCH, WBCH and NCBH fragments. CBCH failed to interact with PS, indicating a requirement for the catalytic DH-PH domains, whereas the absence of the proline-rich motif in the PP, α-HEL and ΔC fragments resulted in a loss of binding to WBCH and NBCH. Furthermore, NBCH demonstrated weak interactions with CT when compared with the full-length and PS constructs. These results suggest that the 45 amino acid overlap present in WBCH, but not NBCH, is not essential for interaction with the proline-rich motif, but may instead, stabilize association of BNIPXL N-terminus with proto-Lbc. This is consistent with the observation that the CBCH domain, which contains the 45 amino acid overlap does not bind to PS. Collectively, our results demonstrate that full-length BNIPXL targets proto-Lbc at its catalytic DH-PH domains and the proline-rich motif (Fig. 6F).

Although both RhoA and RhoC demonstrate an ability to induce stress fibers, RhoA participates in oncogenic transformation differently to RhoC, which promotes cell migration and tumor metastasis (Aspenström et al., 2004). Oncogenic transformation is largely attributed to deregulated RhoGEF signaling (Rossman et al., 2005). The loss of C-terminal regulatory sequences in proto-Lbc results in an increasingly cytosolic distribution and oncogenicity, even though the catalytic activities of proto- and onco-Lbc in vivo remain comparable (Sterpetti et al., 1999). To determine the effects of BNIPXL on the transforming activity of onco-Lbc in NIH3T3 fibroblasts, transient transformation assays were performed using DsRed-onco-Lbc and GFP-BNIPXL (Fig. 6G). The CBCH domain abrogates onco-Lbc transformation whereas full-length BNIPXL exhibits moderate attenuation (25%) – a profile very similar to the enhanced binding of CBCH to RhoA when compared with full-length (Fig. 3A). This suggests that the CBCH domain alone is a potent inhibitor of onco-Lbc transformation. Interestingly, the WBCH domain also downregulates the transforming activity (55%). It is possible that the WBCH domain may function in parallel pathways to suppress Lbc via its binding to the proline-rich motif of Lbc, but independently of RhoA downregulation. Taken together, our results suggest that BNIPXL downregulates RhoA activity and transformation through sequestration of RhoA and Lbc, which together restrict sustained RhoA activation.

Discussion

Although Rho-GTPases serve as universal molecular switches for the cytoskeletal network and are tightly controlled by key regulators such as GAPs, GEFs and GDIs, it remains relatively unknown how the activity of these regulators on their cognate GTPases are regulated by additional cellular protein(s). In the current study, we have identified BNIPXL as a novel regulator for both RhoA and its specific RhoGEF, proto-Lbc, leading to RhoA inactivation and

Journal of Cell Science

Fig. 6. BNIPXL targets proto-Lbc via two distinct sites and suppresses Lbc-induced cellular transformation. (A) Schematic diagram of proto-Lbc and its truncation mutants. α-HEL, α-helical region; PP, proline-rich motif; CT, extreme C-terminus; ΔC, oncogenic Lbc. Lysates expressing Flag-proto-Lbc, mutants or vector control with HA-BNIPXL (B) full-length, (C) CBCH, (D) WBCH or (E) NBCH were subjected to immunoprecipitation and bound proteins detected with anti-HA (first panels) and anti-Flag (second panels) to show the amounts of precipitated proteins. Expression of BNIPXL (third panels) and proto-Lbc (fourth panels) was verified. Asterisks indicate position of the expected band. Arrow indicates the position of the nonspecific bands arising from anti-HA antibody. (F) Schematic diagram indicating a requirement for the DH-PH domains and the proline-rich motif for BNIPXL-Lbc interactions. (G) NIH3T3 was transfected with DsRed-onco-Lbc and GFP-BNIPXL fragments in primary focus formation. Foci were stained with crystal violet after 21 days and the number of foci was counted. Transforming activity of onco-Lbc was set at 100%. Data are means ± s.d. (n=3). Differences between values not sharing the same letters (a, b, c, d) are statistically significant at P<0.05 by analysis of variance and the Student-Newman-Keuls multiple range test (Statgraphics).

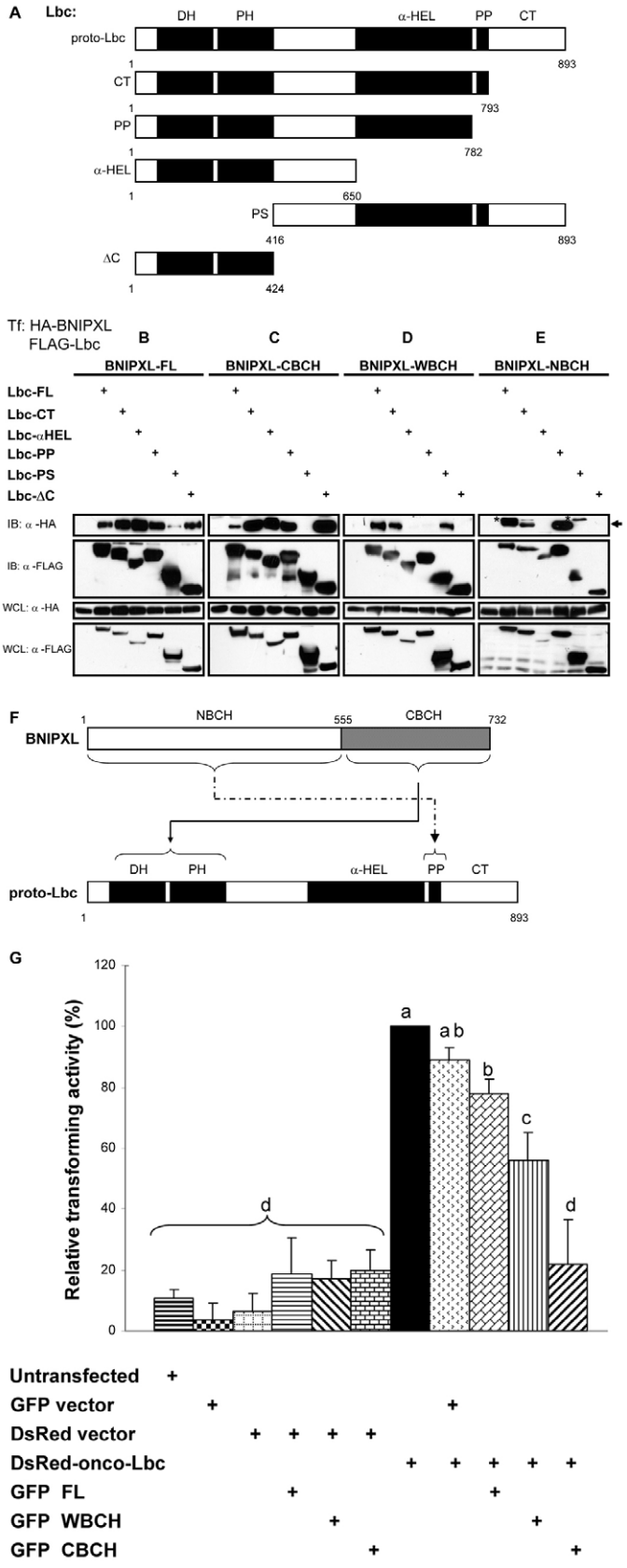

suppression of cellular transformation. As BNIPXL represents a single contig of *BMCC1* that is a favorable prognostic marker for childhood neuroblastomas, this finding could also provide a general model by which BNIPXL or BMCC1 could function as an antagonist of RhoA- and Lbc-induced oncogenicity.

BNIPXL inhibits RhoA-Lbc interaction by separately binding to their different motifs

One unique feature of BNIPXL is its capacity to interact with Rho and RhoGEF, which both require at least the functional BCH domain. Our competition studies demonstrate that such bimodal interactions essentially deprive RhoA and Lbc from interacting with one another, thus effectively shutting off Lbc signaling to RhoA (data not shown). These distinctive interactions are mediated by the BCH domain recognizing RhoA conformational changes or through targeting the catalytic DH-PH domains of Lbc. An additional region(s) at the N-terminus of BNIPXL is also involved in binding to the proline-rich motif of Lbc. These interactions together provide a general mechanism to regulate Lbc-Rho pathways specifically (Fig. 7) and GTPase signaling in general. The motifs responsible for BNIPXL binding to RhoA are likely to be multiple ones, because short internal deletions have all led to complete loss of RhoA binding. Furthermore, the BCH domain exerted greater potency in suppressing Lbc transformation when compared with the full-length protein, consistent with its enhanced binding to RhoA.

BNIPXL is specific towards subtypes and conformational states of Rho

The unique binding profile of BNIPXL to specific RhoA mutants supports our model, which proposes that the BCH domain sequesters both RhoA and Lbc to limit their activation. The ability of BNIPXL to distinguish different RhoA conformations in vivo suggests that BNIPXL is likely to sequester and retain GDP-RhoA in a complex. Future work will determine whether Gly14 (within the P-loop) and Glu63 (within Switch II) could indeed constitute key binding residues for BNIPXL interaction. In addition, we cannot exclude the possibility that BNIPXL could directly promote intrinsic GTPase activity. Alternatively, it may do so through the recruitment of inactivators, such as the BCH-containing Cdc42GAP/p50RhoGAP or BPGAP1, through heterophilic BCH interactions. Similarly, because Lbc distribution contributes to sustained RhoA activation and oncogenic transformation (Sterpetti et al., 1999), BNIPXL could reduce ectopic GEF activation by affecting Lbc localization.

Although the role of Rho-mediated cytoskeletal rearrangements in cellular transformation remains unclear, early studies suggest that

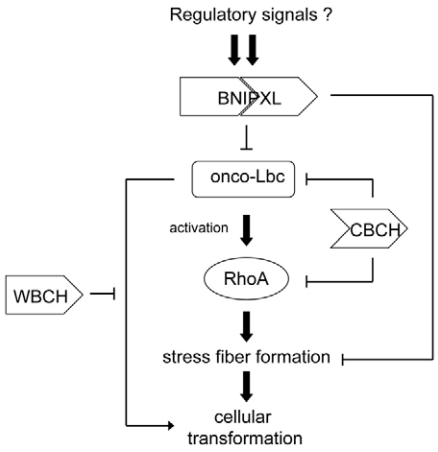

Fig. 7. Proposed roles of BNIPXL in regulating Lbc-RhoA-mediated stress fiber formation and cellular transformation. BNIPXL exerts distinct roles in regulating RhoA pathways that are linked to actin cytoskeleton reorganization and oncogenic transformation. The BNIPXL BCH domain targets RhoA via preferential GDP-RhoA binding and also by sequestering the RhoA upstream activator Lbc by targeting its catalytic DH-PH domains. In addition, the N-terminus devoid of the BCH domain, binds to the proline-rich moiety in the C-terminus regulatory region of proto-Lbc. In a concerted manner, these interactions lead to the disruption of stress fibers and suppression of Lbc-induced cellular transformation. This provides further evidence that BCH domain acts as a regulatory GTPase-binding module that targets both small GTPases and their immediate regulators (see text for details).

Rho promotes two independent pathways, leading to stress fiber formation and oncogenic Ras transformation (Qiu et al., 1995). Activation of p160ROCK, which is necessary for stress fiber formation (Amano et al., 1997), is required (Sahai et al., 1999), but not sufficient for Rho transformation. Rho contributes to transformation through cell growth regulation and survival (Jaffe and Hall, 2002). More significantly, cells transformed by RhoGEFs, including Lbc, retain normal stress fibers (Zheng et al., 1995). Collectively, these results suggest that BNIPXL targets distinct RhoA pathways, including stress fiber assembly and transformation, and is consistent with its function as an antagonist for cell growth in fibroblasts as reported here, or as a pro-apoptotic factor in neuronal cells (Machida et al., 2006). The identification of a specific BNIPXL mutant that uncouples GEF interactions while retaining RhoA binding should address the specific contributions of BNIPXL in linking actin cytoskeleton rearrangements and oncogenic transformation.

Intriguingly, the BNIPXL BCH domain specifically targets RhoA and RhoC, but not RhoB. Despite having similar subcellular distribution and the ability to induce stress fibers (Aspenström et al., 2004; Adamson et al., 1992), current literature suggests that RhoA participates in cellular transformation whereas RhoC promotes tumor metastasis and cell migration (Wang et al., 2003; Wu et al., 2004; Ridley, 2004; Hakem et al., 2005). Interestingly, Lbc demonstrates comparable GEF activity toward RhoA, RhoB and RhoC (Zheng et al., 1995), but their distinct functions remain unknown. Similarly, the role of RhoC in oncogenic Lbc transformation is not well defined and warrants further investigation, especially in light of its specificity in BNIPXL binding. It is interesting to note that BNIPXL overexpression is not associated with profound cell rounding despite Rho inactivation, suggesting that indirect activation of other GTPases such as Rac and Cdc42 lead to the subtle short protrusions observed in the current study. Such multitude of GTPases crosstalking downstream of BNIPXL awaits further investigation.

The BCH domain as a regulatory domain for small GTPases and their regulators

Our current results indicate that a number of motifs within the BCH domain mediate RhoA interaction, in contrast to the involvement of a single GTPase-binding motif within the BCH domains of BNIP2 and BNIP-Sα for targeting Cdc42 and RhoA, respectively. Significantly, only BNIPXL and BNIP-Sα interact with proto-Lbc amongst the four closely related BNIP2 family proteins. Our group has previously shown that BNIP-Sα can displace Cdc42GAP/p50-RhoGAP from RhoA to elicit RhoA activation and pro-apoptotic events. This implies that unlike BNIPXL, which acts by sequestering Lbc and RhoA separately, leading to RhoA inactivation, BNIP-Sα could instead provide a scaffold for Lbc to activate RhoA. This suggests that homologous BCH domains target specific GTPases and their regulators through a common sequestration mechanism to elicit different cellular outcomes. Collectively, our current findings provide further compelling evidence that the BCH domain is an emerging class of regulatory GTPase-binding domain.

DH-PH domains: a common target for specific BCH or Sec14p-like domains?

In addition to Lbc, BNIPXL also targets p115RhoGEF (supplementary material Fig. S7), another RhoA-specific GEF (Hart et al., 1996). By engaging many RhoGEFs, BNIPXL could exert varying levels of inhibition at different RhoA activation nodes. This leads to our hypothesis that BNIPXL may also target p115RhoGEF via the DH-PH domains. If so, the DH-PH domains could become a new target for selective members of the BNIP2 family, in addition to their small GTPase targets. Intriguingly, the BNIPXL BCH domain shares 17% identity (40% similarity) to the yeast Sec14p lipid-binding domain, and our extensive phylogenetic analyses indicate their likely divergence from a common ancestral domain, with many previously annotated or uncharacterized ‘Sec14p-like’ domains in eukaryotic proteins presenting similar features to the BNIP2 family. These include their ability to form homo- and heterophilic interactions and a selectivity for small GTPases (Zhou and Low, manuscript in preparation). In this regard, recent reports demonstrate that resident Sec14p-like domains target Dbl, Ost (Ueda et al., 2004) and Dbs to Golgi membranes while mediating intramolecular interactions with the PH domain to negatively regulate Dbs transforming activity (Kostenko et al., 2005). These findings provide insight into the regulatory role of the Sec14p-like domain for GEF regulation through *cis*-inhibitory interactions. This mechanism is consistent with the role of the BNIPXL BCH domain in sequestering Lbc, and possibly p115RhoGEF via their DH-PH domains by interacting in *trans*. This is in line with previous studies demonstrating that the Lbc DH domain is essential for stress fiber formation but insufficient for efficient transformation, requiring the PH domain for targeting to punctate structures along the stress fibers (Olson et al., 1997). An alignment of the BCH domains of BNIPXL and BNIP2 with the Sec14p-like domains from Dbl, Ost, Dbs and the Sec14p lipid-binding domain indicates that they do indeed exhibit significant homology in several regions (supplementary material Fig. S8). This could pinpoint conserved motifs that execute similar regulatory functions. Therefore, it remains an exciting prospect to investigate whether other BCH or Sec14p-like domains have the capacity to

Journal of Cell Science

target the tandem DH-PH moiety in selective members of the Dbl family GEFs.

Taken together, our findings provide a new line of evidence that BNIPXL could suppress RhoA signaling through concerted mechanisms that target both Rho and its upstream activators, all via unique motifs in its BCH domain, leading ultimately to suppression of cellular transformation. Therefore, the BCH and Sec14p-like domain families represent a novel class of regulators for small GTPases and their cognate regulators, adding greater plasticity to cellular responses mediated by these molecular switches.

Materials and Methods

Antibodies and reagents

Anti-Lbc antiserum was provided by D. Toksoz (Tufts University School of Medicine, Boston, MA). Anti-Flag, TRITC-conjugated phalloidin, goat anti-mouse and anti-rabbit horseradish peroxidase-conjugated secondary antibodies were from Sigma. Anti-c-Myc 9E10, polyclonal anti-RhoA and anti-Cdc42 antibodies were from Santa Cruz Biotechnology. Polyclonal anti-HA was from Zymed Laboratories. FITC-conjugated goat anti-mouse IgG was from Jackson ImmunoResearch Laboratories and glutathione-Sepharose beads were from Amersham Biosciences.

Expression constructs

The pGEX-RhoA, pGEX-Cdc42, pRK5-Myc-p115RhoGEF, Myc-Lbc and Myc-LbcΔC constructs were provided by A. Hall (Memorial Sloan-Kettering Cancer Center, New York, NY). pCAG-Myc-p160ROCK was provided by S. Narumiya (Kyoto University, Japan) while pGEX-Rhotekin-RBD was courtesy of S. Schoenwaelder (Monash University, Australia). pCAGGS-BMCC1-Flag was provided by A. Nakagawara (Chiba Cancer Center Research Institute, Japan). pXJ40-HA-RhoA, RhoB and RhoC was provided by Y. T. Zhou (National University of Singapore, Singapore). BNIPXL truncations were generated by incorporating *Xho*I (forward) and *Not*I (reverse) sites and BNIPXL deletion mutants were generated by site-directed mutagenesis incorporating *Nhe*I and cloned into Flag-, HA- and GFP-pXJ40 mammalian expression vectors provided by E. Manser (Institute of Molecular and Cell Biology, Singapore). pRK5-myc-Lbc and LbcΔC were subcloned into Flag- and DsRed-pXJ40. Proto-Lbc truncation mutants incorporating *Bam*HI was generated as previously described (Sterpetti et al., 1999). Constructs were sequenced to confirm sequence fidelity.

Bioinformatics

Novel BCH-domain-containing proteins were identified using the PSI-BLAST program (Altschul et al., 1997) against the non-redundant and EST databases, as described previously (Low et al., 2000b). Multiple sequence alignments were generated by ClustalW (http://www.ebi.ac.uk/clustalw/) and formatted by BOXSHADE (http://bioweb.pasteur.fr/seqanal/interfaces/boxshade.html#fmtseq). Genome analysis was generated using the Human Genome BLAST (http://www.ncbi.nlm.nih.gov/genome/seq/BlastGen/BlastGen.cgi?taxid=9606).

Cloning and semi-quantitative RT-PCR

BNIPXL cDNA was amplified from human adult brain and kidney libraries (Clontech) using Expand Long Template PCR System (Roche Molecular Biochemicals), with 94°C for 4 minutes, 55°C for 30 seconds and 68°C for 4 minutes, followed by 30 cycles of 94°C for 40 seconds, 55°C for 30 seconds, 68°C for 4 minutes and a final extension of 68°C for 10 minutes. Primers used were full-length forward, 5′-ATGGCTTTGTTTGATGGTGATCC-3′ and reverse, 5′-CTTCTTCCAGCATG-GCCAACTAAGGC-3′. For RT-PCR, 3 μg total RNA [RNeasy Mini Kit (Qiagen)] was used for oligo(dT)-primed first-strand cDNA synthesis with AMV reverse transcriptase (Promega) and further amplified with DyNAzyme (Finnzymes). Primers used were BCH forward, 5′-ATCATTGTGTTTGCCGCCTG-3′ and full-length reverse. Expression was normalized against GAPDH and verified in at least two independent experiments. The *H. sapiens BNIPXL*α and *BNIPXL*β sequences are deposited under accession numbers AY439213 and AY439214, respectively.

Cell culture and transfection

HEK293T, MCF-7 and SK-BR3 were maintained in RPMI-1640 (Hyclone) with 10% FCS (Invitrogen), 2 mM L-glutamine, 100 U/ml penicillin and 100 μg/ml streptomycin (Hyclone). HeLa and MDA-MB-231 cells were maintained in high-glucose DMEM with 0.1 mM NEAA and 1 mM sodium pyruvate (Invitrogen). NIH3T3 cells were maintained in high-glucose DMEM with 10% bovine serum (Invitrogen) and 1.5 g/l sodium bicarbonate. All cells were grown at 37°C, 5% CO_2. HEK293T and HeLa cells were transfected using FuGENE 6 (Roche Molecular Biochemicals) whereas NIH3T3 cells were transfected with Lipofectamine 2000 (Invitrogen).

Immunofluorescence

HeLa cells were processed 24 hours post transfection as previously described (Lua and Low, 2004). Confocal images were captured on Olympus FluoView FV500 microscope with a 60× oil-immersion lens. NIH3T3 cells were starved 24 hours post-transfection for 16 hours and stimulated with growth medium containing 0.5% serum for 10 minutes to induce stress fibers, according to Ridley and Hall (Ridley and Hall, 1992). Cells were fixed, stained and examined by indirect immnofluorescence. Fluorescence images were captured on Zeiss LSM510 META microscope using a 60× water-immersion lens. The percentage of transfected cells exhibiting stress fibers was evaluated for quantitative analysis of stress fiber assembly. At least 100 transfected cells per construct were evaluated for stress fiber assembly. Data are means ± s.d. from three independent experiments. Statistical significance was analyzed using ANOVA and the Student-Newman-Keuls multiple range test (Statgraphics).

Coimmunoprecipitation and western blotting

HEK293T cells were lysed (50 mM HEPES, pH 7.4, 150 mM sodium chloride, 1.5 mM magnesium chloride, 5 mM EGTA, 10% glycerol, 1% Triton X-100, 5 mM sodium orthovanadate, and a mixture of protease inhibitors) and directly analyzed as whole-cell lysates or aliquots used for affinity precipitation with anti-Flag M2 Affinity Gel (Sigma), as previously described (Low et al., 2000a). Bound proteins were eluted and separated by SDS-PAGE for western analyses. For partial endogenous immunoprecipitation, cells were lysed in NP-40 lysis buffer (50 mM Tris-HCl pH 8.0, 150 mM sodium chloride, 1% Nonidet P-40 and a mixture of protease inhibitors). 5 mg total protein was subjected to immunoprecipitation with anti-Flag M2 Affinity Gel overnight at 4°C and processed as described (Park et al., 2002).

Direct protein-binding assays

GST fusion proteins were purified from *E. coli* BL21(DES) (Shang et al., 2003). In-vitro-transcribed and translated Flag-tagged proteins were synthesized [TNT Quick Coupled Transcription/Translation System (Promega)], and aliquots incubated with GST-RhoA (10 μg) overnight at 4°C. Samples were diluted with 100 μl cell lysis buffer and incubated for 1 hour at 4°C. Beads were washed three times with cell lysis buffer and bound proteins separated by SDS-PAGE for western analyses.

In vitro GTP and GDP loading assays

GST-RhoA (10 μg) were preloaded with 10 mM GDP or GTPγS (Sigma) in binding buffer (25 mM NaCl, 20 mM Tris-HCl pH 7.5, 0.1 mM DTT) and 50 mM EDTA at 30°C for 10 minutes. The reaction was stopped with $MgCl_2$ to a final concentration of 20 mM (Ren and Schwartz, 2000). The beads were incubated with lysates at 4°C in GAP lysis buffer (50 mM HEPES pH 7.4, 150 mM NaCl, 1.5 mM $MgCl_2$, 5 mM EGTA, 10% glycerol, 1% Triton X-100, 5 mM sodium orthovanadate and a mixture of protease inhibitors) and washed with immunoprecipitation wash buffer (20 mM HEPES pH 7.4, 150 mM NaCl, 10 mM $MgCl_2$, 10% glycerol, 0.1% Triton X-100). Bound proteins were separated by SDS-PAGE for western analyses.

RhoA activation assays

HEK293T cells were lysed in lysis buffer (50 mM Tris-HCl pH 7.4, 2 mM magnesium chloride, 1% Triton X-100, 10% glycerol, 100 mM sodium chloride, supplemented with 1 mM DTT and a mixture of protease inhibitors) and 300 μg lysates was incubated with GST-Rhotekin-RBD for 30 minutes at 4°C (Besson et al., 2004). The beads were washed three times with lysis buffer and bound proteins separated by SDS-PAGE for western blot analyses.

Short-hairpin RNA (shRNA) knockdown

Six shRNA oligonucleotides against human *BNIPXL* were designed using the siRNA target finder (Ambion), synthesized (Operon) and cloned into the pSilencer 2.1-U6 hygro vector (Ambion). The shRNA sequences are sh473, 5′-GATCCCATGCTTTCACCACAGCCTGTTCAAGAGACAGGCTGTGGTGAA-AGCATTTTTTTGGAAA-3′; sh477, 5′-GATCCCGTGACACTCATCCTCGGA-GATTCAAGAGATCTCCGAGGATGAGTGTCATTTTTTGGAAA-3′; sh479, 5′-GATCCCACAATAGAGGAAGCTGGGTTTCAAGAGAACCCAGCTTCCTCT-ATTGTTTTTTTGGAAA-3′; sh47C, 5′-GATCCCGAGCAGCGCATTGACATG-ATTCAAGAGATCATGTCAATGCGCTGCTCTTTTTTGGAAA-3′; sh470, 5′-GATCCGCGCATTGACATGAAGGTCATCTCGAGATGACCTTCATGTCAATG-CGCTTTTTTGGAAA-3′; sh484, 5′-GATCCGCCAACAAAGATTCTGGCCA-ACTCGAGTTGGCCAGAATCTTTGTTGGCTTTTTTGGAAA-3′. Constructs were sequenced to confirm sequence fidelity and knockdown efficiency was determined by cotransfection with GFP- or HA-BNIPXL plasmid at a 10:1 ratio. Lysates were analyzed 72 hours post transfection.

Transformation assays

Primary focus formation assays were performed in NIH3T3 cells using calcium phosphate precipitation (Solski et al., 2000). NIH3T3 cells seeded at 2.5×10^5 cells/60 mm dish were cotransfected with DsRed-LbcΔC and GFP-BNIPXL, GFP-WBCH or GFP-CBCH and grown in complete medium. Cells were fixed (10% acetic acid, 10% methanol), stained with 0.5% Crystal Violet and foci formation was scored 21 days post transfection. Each experiment was performed at least three times. Data were analyzed for statistical significance using ANOVA and the Student-Newman-Keuls multiple range test (Statgraphics).

Journal of Cell Science

We thank A. Hall (Memorial Sloan-Kettering Cancer Center, USA), S. Narumiya (Kyoto University, Japan), S. Schoenwaelder (Monash University, Australia), D. Toksoz (Tufts University School of Medicine, USA) and A. Nakagawara (Chiba Cancer Center Research Institute, Japan) for generous gifts of plasmid constructs and antisera. We thank the National University Medical Institutes for the use of confocal microscopy units, Chew Li Li for helpful discussions and Aarthi Ravichandran for critical review of our manuscript. This work is supported in part by a grant from Biomedical Research Council of Singapore and the BMRC Young Investigator Award to B.C.L.

References

Adamson, P., Paterson, H. F. and Hall, A. (1992). Intracellular localization of the P21rho proteins. *J. Cell Biol.* **119**, 617-627.

Altschul, S. F., Madden, T. L., Schaffer, A. A., Zhang, J., Zhang, Z., Miller, W. and Lipman, D. J. (1997). Gapped BLAST and PSI-BLAST: a new generation of protein database search programs. *Nucleic Acids Res*. **25**, 3389-3402.

Amano, M., Chihara, K., Kimura, K., Fukata, Y., Nakamura, N., Matsuura, Y. and Kaibuchi, K. (1997). Formation of actin stress fibers and focal adhesions enhanced by Rho-Kinase. *Science* **275**, 1308-1311.

Aspenström, P., Fransson, Å. and Saras, J. (2004). Rho GTPases have diverse effects on the organization of the actin filament system. *Biochem. J.* **377**, 327-337.

Besson, A., Gurian-West, M., Schmidt, A., Hall, A. and Roberts, J. M. (2004). p27Kip1 modulates cell migration through the regulation of RhoA activation. *Genes Dev*. **18**, 862-876.

Boettner, B. and van Aelst, L. (2002). The role of Rho GTPases in disease development. *Gene* **286**, 155-174.

Bos, J. L., Rehmann, H. And Wittinghofer, A. (2007). GEFs and GAPs: critical elements in the control of small G proteins. *Cell* **129**, 865-877.

Buschdorf, J. P., Chew, L. L., Zhang, B., Cao, Q., Liang, F. Y., Liou, Y. C., Zhou, Y. T. and Low, B. C. (2006). Brain-specific BNIP-2-homology protein Caytaxin relocalises glutaminase to neurite terminals and reduces glutamate levels. *J. Cell Sci.* **119**, 3337-3350.

Dvorsky, R. and Ahmadian, M. R. (2004). Always look on the bright side of Rho: structural implications for a conserved intermolecular interface. *EMBO Rep*. **5**, 1130-1136.

Etienne-Manneville, S. and Hall, A. (2002). Rho GTPases in cell biology. *Nature* **420**, 629-635.

Fernandez-Borja, M., Janssen, L., Verwoerd, D., Hordijk, P. and Neefjes, J. (2005). RhoB regulates endosome transport by promoting actin assembly on endosomal membranes through Dia1. *J. Cell Sci*. **118**, 2661-2670.

Fujisawa, K., Madaule, P., Ishizaki, T., Watanabe, G., Bito, H., Saito, Y., Hall, A. and Narumiya, S. (1998). Different regions of Rho determine Rho-selective binding of different classes of Rho target molecules. *J. Biol. Chem*. **273**, 18943-18949.

Glaven, J. A., Whitehead, I. P., Nomanbhoy, T., Kay, R. and Cerione, R. A. (1996). Lfc and Lsc oncoproteins represent two new guanine nucleotide exchange factors for the Rho GTP-binding protein. *J. Biol. Chem*. **271**, 27374-27381.

Hakem, A., Sanchez-Sweatman, O., You-Ten, A., Duncan, G., Wakeham, A., Khokha, R. and Mak, T. W. (2005). RhoC is dispensable for embryogenesis and tumor initiation but essential for metastasis. *Genes Dev*. **19**, 1974-1979.

Hall, A. (1998). Rho GTPases and the actin cytoskeleton. *Science* **279**, 509-514.

Hart, M. J., Eva, A., Zangrilli, D., Aaronson, S. A., Evans, T., Cerione, R. A. and Zheng, Y. (1994). Cellular transformation and guanine nucleotide exchange activity are catalyzed by a common domain on the dbl oncogene product. *J. Biol. Chem.* **269**, 62-65.

Hart, M. J., Sharma, S., elMasry, N., Qiu, R. G., McCabe, P., Polakis, P. and Bollag, G. (1996). Identification of a novel guanine nucleotide exchange factor for the Rho GTPase. *J. Biol. Chem.* **271**, 25452-25458.

Ishizaki, T., Maekawa, M., Fujisawa, K., Okawa, K., Iwamatsu, A., Fujita, A., Watanabe, N., Saito, Y., Kakizuka, A., Morii, N. et al. (1996). The small GTP-binding protein Rho binds to and activates a 160 kDa Ser/Thr protein kinase homologous to myotonic dystrophy kinase. *EMBO J.* **15**, 1885-1893.

Jaffe, A. B. and Hall, A. (2002) RhoGTPases in transformation and metastasis. *Adv. Cancer Res.* **84,** 57-80.

Jaffe, A. B. and Hall, A. (2005). Rho GTPases: biochemistry and biology. *Annu. Rev. Cell Dev. Biol.* **21**, 247-269.

Kostenko, E. V., Mahon, G. M., Cheng, L. and Whitehead, I. P. (2005). The Sec14 Homology domain regulates the cellular distribution and transforming activity of the Rho-specific guanine nucleotide exchange factor Dbs. *J. Biol. Chem.* **280**, 2807-2817.

Lin, R., Cerione, R. A. and Manor, D. (1999). Specific contributions of the small GTPases Rho, Rac, and Cdc42 to Dbl transformation. *J. Biol. Chem.* **274**, 23633-23641.

Low, B. C., Lim, Y. P., Lim, J., Wong, E. S. and Guy, G. R. (1999). Tyrosine phosphorylation of the Bcl-2-associated protein BNIP-2 by fibroblast growth factor receptor-1 prevents its binding to Cdc42GAP and Cdc42. *J. Biol. Chem.* **274**, 33123-33130.

Low, B. C., Seow, K. T. and Guy, G. R. (2000a). Evidence for a novel Cdc42GAP domain at the carboxyl terminus of BNIP-2. *J. Biol. Chem.* **275**, 14415-14422.

Low, B. C., Seow, K. T. and Guy, G. R. (2000b). The BNIP-2 and Cdc42GAP homology domain of BNIP-2 mediates its homophilic association and heterophilic interaction with Cdc42GAP. *J. Biol. Chem.* **275**, 37742-33751.

Lua, B. L. and Low, B. C. (2004). BPGAP1 interacts with cortactin and facilitates its translocation to cell periphery for enhanced cell migration. *Mol. Biol. Cell* **15**, 2873-2883.

Lua, B. L. and Low, B. C. (2005). Activation of EGF receptor endocytosis and ERK1/2 signaling by BPGAP1 requires direct interaction with EEN/endophilin II and a functional RhoGAP domain. *J. Cell Sci.* **118**, 2707-2721.

Machida, T., Fujita, T., Ooo, M. L., Ohira, M., Isogai, E., Mihara, M., Hirato, J., Tomotsune, D., Hirata, T., Fujimori, M. et al. (2006). Increased expression of proapoptotic BMCC1, a novel gene with the BNIP2 and Cdc42GAP homology (BCH) domain, is associated with favorable prognosis in human neuroblastomas. *Oncogene* **25**, 1931-1942.

Moon, S. Y. and Zheng, Y. (2003). Rho GTPase-activating proteins in cell regulation. *Trends Cell Biol.* **13**, 13-22.

Nagase, T., Ishikawa, K., Nakajimam, D., Ohiram, M., Sekim, N., Miyajimam, N., Tanaka, A., Kotani, H., Nomura, N. and Ohara, O. (1997). Prediction of the coding sequences of unidentified human genes. VII. The complete sequences of 100 new cDNA clones from brain which can code for large proteins in vitro. *DNA Res.* **28**, 141-150.

Olson, M., Sterpetti, P., Nagata, K., Toksoz, D. and Hall, A. (1997). Distinct roles for DH and PH domains in the *lbc* oncogene. *Oncogene* **15**, 2827-2832.

Qiu, R., Chen, J., McCormick, F. and Symons, M. (1995). A role for Rho in Ras transformation. *Proc. Natl. Acad. Sci. USA* **92**, 11781-11785.

Park, B., Nguyen, N. T., Dutt, P., Merdek, K. D., Bashar, M., Sterpetti, P., Tosolini, A., Testa, J. R. and Toksoz, D. (2002). Association of Lbc Rho GEF with alpha-catenin-related protein, alpha-catulin/CTNNAL1, supports serum response factor activation. *J. Biol. Chem.* **277**, 45361-45370.

Ren, X. D. and Schwartz, M. A. (2000). Determination of GTP-loading on Rho. *Meth. Enzymol.* **325**, 264-272.

Ridley, A. (2004). Rho proteins and cancer. *Breast Cancer Res. Treat*. **84**, 13-19.

Ridley, A. J. and Hall, A. (1992). The small GTP-binding protein rho regulates the assembly of focal adhesions and actin stress fibers in response to growth factors. *Cell* **70**, 389-399.

Rossman, K. L., Der, C. J. and Sondek, J. (2005). GEF means go: turning on Rho GTPases with guanine nucleotide-exchange factors. *Nat. Rev. Mol. Cell Biol*. **6**, 167-180.

Sahai, E. and Marshall, C. J. (2002). RHO-GTPases and cancer. *Nat. Rev. Cancer* **2**, 133-142.

Sahai, E., Ishizaki, T., Narumiya, S. and Treisman, R. (1999). Transformation mediated by RhoA requires activity of ROCK kinases. *Curr. Biol.* **11**, 136-145.

Shang, X., Zhou, Y. T. and Low, B. C. (2003). Concerted regulation of cell dynamics by BNIP-2 and Cdc42GAP homology/Sec14p-like, proline-rich, and GTPase-activating protein domains of a novel Rho GTPase-activating protein, BPGAP1. *J. Biol. Chem.* **278**, 45903-45914.

Solski, P. A., Abe, K. and Der, C. J. (2000). Analyses of transforming activity of Rho family activators. *Meth. Enzymol. 325*, 425-441.

Sterpetti, P., Hack, A. A., Bashar, M. P., Park, B., Cheng, S. D., Knoll, J. H. M., Urano, T., Feig, L. A. and Toksoz, D. (1999). Activation of the Lbc Rho exchange factor proto-oncogene by truncation of an extended C terminus that regulates transformation and targeting. *Mol. Cell. Biol.* **19**, 1334-1345.

Tcherkezian, J. and Lamarche-Vane, N. (2007). Current knowledge of the large RhoGAP family of proteins. *Biol. Cell* **99**, 67-86.

Toksoz, D. and Williams, D. A. (1994). Novel human oncogene *lbc* detected by transfection with distinct homology regions to signal transduction products. *Oncogene* **9**, 621-628.

Ueda, S., Kataoka, T. and Satoh, T. (2004). Role of the Sec14-like domain of Dbl family exchange factors in the regulation of Rho family GTPases in different subcellular sites. *Cell. Signal.* **16**, 899-906.

Wang, L., Yang, L., Luo, Y. and Zheng, Y. (2003). A novel strategy for specifically down-regulating individual Rho GTPase activity in tumor cells. *J. Biol. Chem*. **278**, 44617-44625.

Wheeler, A. P. and Ridley, A. (2004). Why three Rho proteins? RhoA, RhoB, RhoC and cell motility. *Exp. Cell Res.* **301**, 43-49.

Whitehead, I., Kirk, H., Tognon, C., Trigo-Gonzalez, G. and Kay, R. (1995). Expression Cloning of lfc, a Novel Oncogene with Structural Similarities to Guanine Nucleotide Exchange Factors and to the Regulatory Region of Protein Kinase C. *J. Biol. Chem.* **270**, 18388-18395

Whitehead, I. P., Khosravi-Far, R., Kirk, H., Trigo-Gonzalez, G., Der, C. J. and Kay, R. (1996). Expression cloning of lsc, a novel oncogene with structural similarities to the Dbl family of guanine nucleotide exchange factors. *J. Biol. Chem.* **271**, 18643-18650.

Wu, M., Wu, Z., Chandan, K., Chinnaiyan, A. and Merajver, S. D. (2004). RhoC induces differential expression of genes involved in invasion and metastasis in MCF10A breast cells. *Breast Cancer Res. Treat.* **84**, 3-12.

Zheng, Y., Olson, M. F., Hall, A., Cerione, R. A. and Toksoz, D. (1995). Direct involvement of the small GTP-binding protein Rho in *lbc* oncogene function. *J. Biol. Chem.* **270**, 9031-9034.

Zhou, Y. T., Soh, U. J., Shang, X., Guy, G. R. and Low, B. C. (2002). The BNIP-2 and Cdc42GAP homology/Sec14p-like domain of BNIP-Salpha is a novel apoptosis-inducing sequence. *J. Biol. Chem.* **277**, 7483-7492.

Zhou, Y. T., Guy, G. R. and Low, B. C. (2005). BNIP-2 induces cell elongation and membrane protrusions by interacting with Cdc42 via a unique Cdc42-binding motif within its BNIP-2 and Cdc42GAP homology domain. *Exp. Cell Res*. **303**, 263-274.

Zhou, Y. T., Guy, G. R. and Low, B. C. (2006). BNIP-Salpha induces cell rounding and apoptosis by displacing p50RhoGAP and facilitating RhoA activation via its unique motifs in the BNIP-2 and Cdc42GAP homology domain. *Oncogene* **25**, 2393-2408.

Journal of Cell Science